ALLOY CATALYSTS WITH MONOLITH SUPPORTS FOR METHANATION OF COAL-DERIVED GASES. QUARTERLY TECHNICAL PROGRESS REPORT, JUNE 21-SEPTEMBER 20, 1979

BRIGHAM YOUNG UNIV.
PROVO, UT

05 OCT 1979

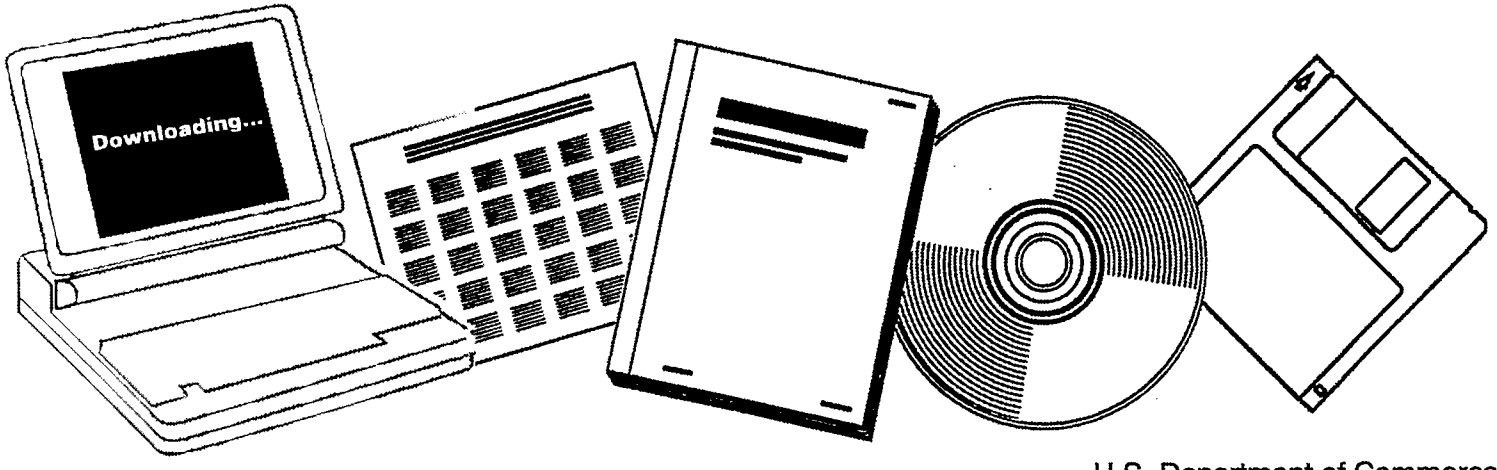

One Source. One Search. One Solution.

NTIS

Providing Permanent, Easy Access to U.S. Government Information

National Technical Information Service is the nation's largest repository and disseminator of government-initiated scientific, technical, engineering, and related business information. The NTIS collection includes almost 3,000,000 information products in a variety of formats: electronic download, online access, CD-ROM, magnetic tape, diskette, multimedia, microfiche and paper.

Search the NTIS Database from 1990 forward

NTIS has upgraded its bibliographic database system and has made all entries since 1990 searchable on **www.ntis.gov.** You now have access to information on more than 600,000 government research information products from this web site.

Link to Full Text Documents at Government Web Sites

Because many Government agencies have their most recent reports available on their own web site, we have added links directly to these reports. When available, you will see a link on the right side of the bibliographic screen.

Download Publications (1997 - Present)

NTIS can now provides the full text of reports as downloadable PDF files. This means that when an agency stops maintaining a report on the web, NTIS will offer a downloadable version. There is a nominal fee for each download for most publications.

For more information visit our website:

www.ntis.gov

U.S. DEPARTMENT OF COMMERCE
Technology Administration
National Technical Information Service
Springfield, VA 22161

FE-2729-8
Distribution Category UC-90e

ALLOY CATALYSTS WITH MONOLITH SUPPORTS FOR METHANATION OF COAL-DERIVED GASES

Quarterly Technical Progress Report
For Period June 21, 1979 to September 20, 1979

Calvin H. Bartholomew
Brigham Young University
Provo, Utah 84602

Date Published -- October 5, 1979

PREPARED FOR THE UNITED STATES
DEPARTMENT OF ENERGY

Under Contract No. EF-77-S-01-2729

FOREWORD

This report summarizes technical progress during the eighth quarter (June 21, 1979 to September 20, 1979) of a two and one-half year study conducted for the Department of Energy (DOE) under Contract No. EF-77-S-01-2729. The principal investigator for this work was Dr. Calvin H. Bartholomew; Dr. Paul Scott was the technical representative for DOE.

The following students contributed to the technical accomplishments and to this report: Erek Erekson, Ed Sughrue, Gordon Weatherbee, Don Mustard, and John Watkins. Mr. Erekson and Dr. Bartholomew were the principal authors. Karen Barrett and Oscar Delgado provided typing and drafting services. In this report data are reported in SI units.

TABLE OF CONTENTS

LIST OF FIGURES

LIST OF TABLES

ABSTRACT

During the eighth quarter kinetic studies of monolithic Ni/Al_2O_3 revealed a shift in activation energy for methanation of CO above 573 K. In kinetic studies at high pressure rapid deactivation was observed for low loading monolithic catalysts. A one-dimensional computer model for methanation over monolithic catalysts was developed to provide insight into experimental conversion vs. temperature data taken in this laboratory. A new method for qualitatively determining sulfur on poisoned catalysts was developed and tested. Metal crystallite size distribution data obtained from transmission electron micrograph (TEM) studies on Ni/silica catalysts suggest that sintering may occur by both crystallite and atomic migration mechanisms. TEM studies of 3% Ni/TiO_2 reveal the presence of raft-like crystallites. These and other accomplishments are reported and discussed.

I. OBJECTIVES AND SCOPE

A. Background

Natural gas is a highly desirable fuel because of its high heating value and nonpolluting combustion products. In view of the expanding demand for and depletion of domestic supplies of clean fuels, economic production of synthetic natural gas (SNG) from coal ranks high on the list of national priorities.

Presently there are several gasification processes under development directed toward the production of SNG. Although catalytic methanation of coal synthesis gas is an important cost item in each process, basic technological and design principles for this step are not well advanced. Extensive research and development are needed before the process can realize economical, reliable operation. Specifically, there appear to be important economical advantages in the development of more efficient, stable catalysts.

From the literature (1,2), three major catalyst problems are apparent which relate to stability: (i) sulfur poisoning, (ii) carbon deposition with associated plugging, and (iii) sintering. Our understanding of these problems is at best sorely inadequate, and the need to develop new and better catalyst technology is obvious. Nevertheless, there has been very little research dealing with new catalyst concepts such as bimetallic (alloy) or monolithic-supported catalysts for methanation. This study deals specifically with sulfur poisoning, carbon deposition, and the effects of support (monolith and pellet) geometry on the performance of alloy methanation catalysts.

B. Objectives

The general objectives of this research program are (i) to study the kinetics of methanation for a few selected catalysts tested during the first two years, (ii) to investigate these catalysts for resistance to deactivation due to sulfur poisoning and thermal degradation. The work is divided into five tasks.

Task 1. Characterize the surface, bulk and phase compositions, surface areas, and metal crystallite sizes for alumina-supported Ni, Ni-Co, Ni-MoO_3, Ni-Pt, Ni-Ru and Ru catalysts.

Task 2. Continue activity testing and support geometry studies of Ni and Ni-bimetallic catalysts initiated during the first two years. The tests include (i) conversion vs. temperature runs at low and high pressures, (ii) steady-state carbon deposition tests, (iii) in situ H_2S tolerance tests, and (iv) support geometry comparisons.

Task 3. Perform kinetic studies to find intrinsic rate data for alumina-supported Ni, Ni-Co, Ni-MoO_3, Ni-Pt, Ni-Ru, and Ru catalysts over a range of pressures and feed compositions. Detailed rate expressions for each catalyst will be determined at low and high pressure.

Effectiveness factors for monolithic and pellet-supported nickel on alumina will be obtained by comparing specific rates to those of finely powdered nickel on alumina.

Task 4. Determine H_2S poisoning rates, thermal deactivation rates, and operating temperature limits for Ni, Ni-Co, Ni-MoO_3, Ni-Pt, Ni-Ru, and Ru catalysts.

Task 5. Continue laboratory visits and technical communications. Interact closely with industrial and governmental representatives to promote large scale testing and development of the two or three best monolithic or pelleted alloy catalysts from this study.

C. Technical Approach

The technical approach which will be used to accomplish the tasks outlined above is presented in the statement of work dated May 20, 1977. The main features of that approach are reviewed here along with more specific details and modifications which have evolved as a result of progress. It is expected that various other aspects of this approach will be modified and improved as the project develops and as new data are made available. Nevertheless, the objectives, tasks and principle features of the approach will remain the substantially the same.

Task 1: Catalyst Characterization

A comprehensive examination of alumina-supported Ni, Ni-Co, Ni-MoO_3, Ni-Pt, Ni-Ru, and Ru catalysts will be carried out to determine surface, bulk, and phase compositions, surface areas, and metal crystallite sizes using the following techniques: chemisorption, x-ray diffraction, chemical analysis, ESCA and SIMS spectroscopy, Auger spectroscopy and transmission electron microscopy.

Hydrogen chemisorption uptakes will be measured using a conventional volumetric apparatus before each reactor test and before and after deactivation tests. X-ray diffraction measurements will be carried out to determine the active metallic phases and metal crystallite size where possible. Selected "aged" samples from Task 4 will be analyzed (by x-ray, chemical analysis, and perhaps ESCA) to determine carbon content and possible changes in phase composition or particle size. Also, transmission electron micrographs will be made to determine particle size distributions for catalyst samples. A few samples will be analyzed by EDAX to determine composition.

Task 2: Activity Testing and Support Geometry Design

Methanation activity and sulfur tolerance measurements initiated during the previous two years of study (3) will be completed. Pellet and monolithic alumina-supported Ni, Ni-Co, Ni-MoO_3, Ni-Pt, Ni-Ru, and Ru catalysts, (both high and low metal loadings) will be activity

tested over a range of temperatures, pressures, and H_2S concentrations. A comparison of steady state conversions for nickel on different pellet and monolith supports of varying geometry will be made. Low pressure activity and sulfur tolerance tests will also be made for pelleted Co/Al_2O_3 and unsupported Ni-Co and Ni-Mo alloys. A summary of the five test procedures and corresponding experimental conditions is listed in Table 1.

Task 3: Kinetic Studies

In order to make more extensive kinetic studies of the six catalyst metal combinations a new mixed flow reactor system will be constructed. This system will be capable of operation to 7500 kPa and 775 K and over a range of reactant compositions. The reactor for this system will be a "Berty" type constant volume mixed flow Autoclave reactor.

Intrinsic rate data will be obtained for alumina-supported Ni, Ni-Co, $Ni-MoO_3$, Ni-Pt, Ni-Ru, and Ru catalysts over a range of pressures and feed compositions in order to obtain detailed rate expressions at low and high pressures. To insure gradientless operation in the reaction-limited regime the rates will be measured at low conversions (0-5%) and low temperatures (525-600 K) for samples which have been crushed to obtain small particles.

Isothermal effectiveness factors for monolithic and pellet-supported nickel on alumina will be obtained by comparing their specific rates to those of finely powdered nickel on alumina using the same mixed flow reactor.

Task 4: Degradation Studies

H_2S poisoning rates and thermal deactivation rates at low pressure will be studied using a new quartz reactor system. Quartz was selected as the material for the reactor because it must operate at high temperatures (750-1000 K) and in a corrosive (H_2S) environment. This reactor is also a constant volume mixed flow type reactor according to the design of Katzer (4). The quartz reactor system will be constructed during the early part of the contract period. Thermal deactivation at high pressures will be studied using a tubular stainless steel reactor previously discussed (3).

Operating temperature limits (and specific reaction rates within this range), thermal deactivation rates near the upper use temperature (in the presence and absence of steam), and H_2S poisoning rates (at 525 K in the presence of 1 and 10 ppm H_2S in H_2) will be determined for Ni, Ni-Co, $Ni-MoO_3$, Ni-Pt, Ni-Ru, and Ru catalysts. The extent of carbon-carbide deposited in the thermal deactivation runs will be determined by chemical analysis and x-ray diffraction.

Table 1

Description of Reactor Tests for Task 2

Test Procedures	Experimental Conditions
1. Temperature-Conversion Test: Measure CO conversion and methane production as a function of temperature, with and without 1% (by vol.) of steam present in the reactant mixture.	475-675 K 140 kPa 30,000 hr^{-1} 1% CO, 4% H_2, 95% N_2 (dry basis)
2. Temperature-Conversion Test (high pressure): Measure CO conversion and methane production as a function of temperature at 2500 kPa.	475-675 K 2500 kPa 30,000 hr^{-1} 1% CO, 4% H_2, 95% N_2
3. Steady State (24 Hr.) Carbon Deposition Test: Measure CO conversion and methane production at 500 and 525 K (250,000 hr^{-1}) before and after an exposure of 24 hours at 675 K.	675 K (24 hrs.) 140 kPa 200,000-250,000 hr^{-1} 25% CO, 50% H_2, 25% N_2
4. In situ H_2S Tolerance Test: Measure intermittently the production of methane and hydrocarbons (by FID) during 24 hours exposure to feed containing 1 or 10 ppm H_2S using a glass reactor.	525 K 140 kPa 30,000 hr^{-1} 1% CO, 4% H_2, 95% N_2 1 or 10 ppm H_2S
5. Support Geometry Tests: Measure CO conversion and methane production as a function of temperature for the same Ni/Al_2O_3 catalyst supported on monoliths and pellets of varying geometries.	575-675 K 140 kPa 30,000 hr^{-1} 1% CO, 4% H_2, 95% N_2

Task 5: Technical Interaction and Technology Transfer

The principal investigator will continue to communicate closely with other workers in methanation catalysis, continue distribution of quarterly reports to selected laboratories to stimulate interest and feedback, attend important coal and catalysis meetings, and visit other methanation laboratories.

He will also interact closely with Mr. A.L. Lee at the Institute of Gas Technology, with personnel at the Pittsburgh Energy Research Center and with other coal gasification representatives to promote large scale testing and development of the two or three best catalysts from this study.

II. SUMMARY OF PROGRESS

A project progress summary is presented in Figure 1 and accomplishments during the past quarter are summarized below. Figure 1 shows that task accomplishments are on schedule. During the past quarter, a contract extension of 6 months was approved.

Accomplishments and results from the past quarter are best summarized according to task:

Task 1. A new method for analyzing sulfur in poisoned catalyst samples was developed during the past quarter. Preliminary tests show excellent results. The stoichiometry of hydrogen adsorption on nickel surfaces was determined to be 1 H per surface Ni atom in agreement with previous work in this laboratory. Preparation and characterization of catalysts by means of hydrogen chemisorption continued. Evidence was obtained from transmission electron microscopy (TEM) that nickel catalyst sintering occurs by both crystallite and atomic migration mechanisms. At higher temperatures atomic migration appears to predominate.

Task 2. No specific progress was made in this task during the past quarter. Activity tests for monolithic catalysts of differing geometry is planned during the next quarter.

Task 3. High pressure kinetic studies in the Berty reactor continued with the testing of several pellet and monolith catalysts. Deactivation of the catalysts at 6900 kPa appears to be caused by heavy hydrocarbons. Also, the activation energy of methanation decreases above 573 K in agreement with work on nickel foils and powders. A computer model to simulate methanation in monolith catalysts at high pressure was developed. Pertinent insights from the computer model regarding the kinetics of methanation are discussed.

Task 4. Experiments performed in this laboratory show that quartz internal recycle reactor developed by Fitzharris and Katzer has application for kinetic and poisoning studies on monolith catalysts. However, for pellets and powders the quartz reactor does not develop sufficient flow through a catalyst bed. A letter submitted to Industrial and Engineering Chemistry: Fundamentals describing the basis for these conclusions is summarized.

Task 5. The principal investigator presented a paper at the International Conference on the Chemistry and Uses of Molybdenum regarding sulfur resistant Ni-Mo catalysts. Six publications are in manuscript preparation based on work from this contract; one paper was submitted and one is in press.

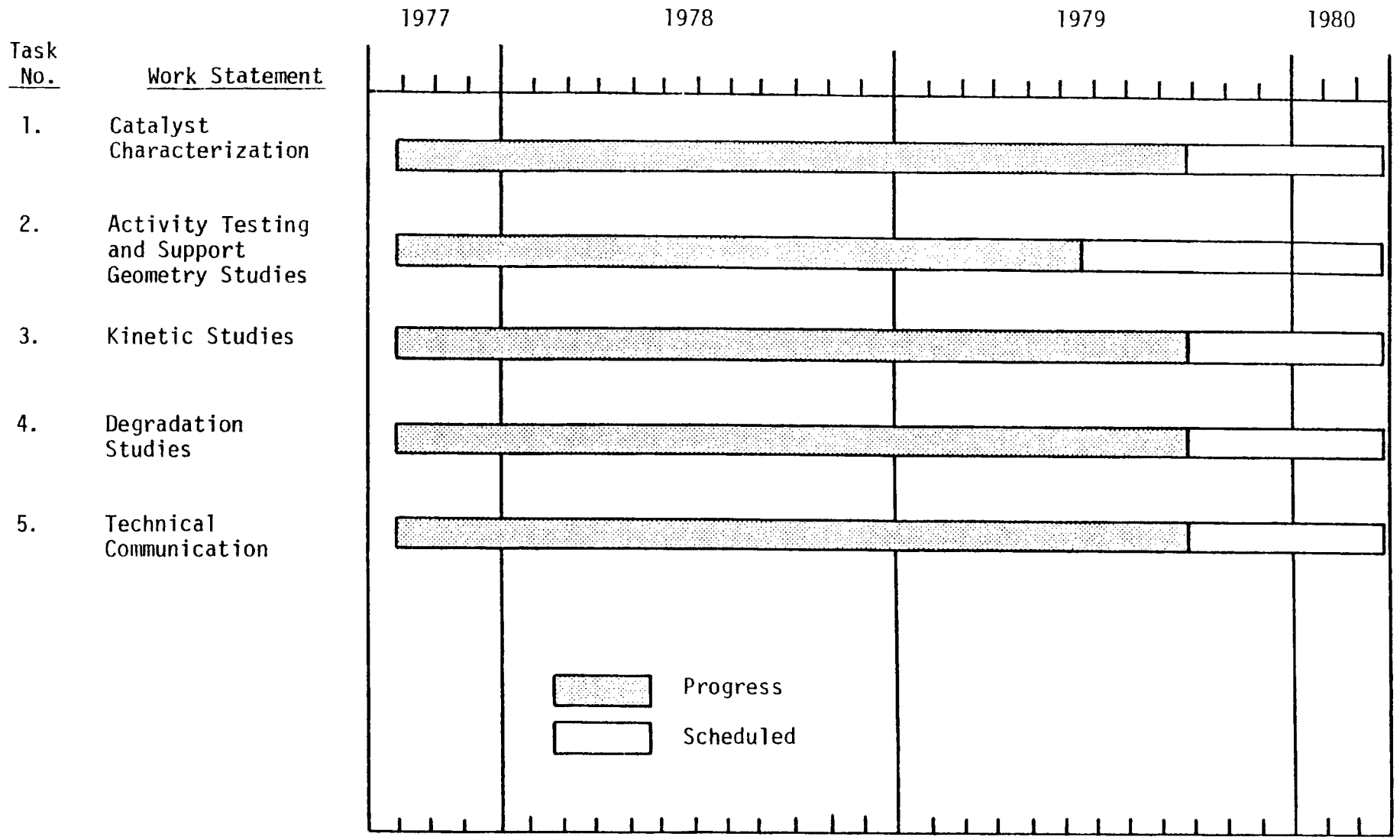

Figure 1. Project Progress Summary

III. DETAILED DESCRIPTION OF TECHNICAL PROGRESS

Task 1: Catalyst Characterization

1. Catalyst Preparation

A series of cordierite monoliths with a 2% alumina washcoat and 0.1% nickel were prepared during the last quarter. In order to minimize metal-support differences, these catalysts have the same nickel to alumina ratio as the 0.5% Ni monoliths previously prepared (5). The 0.1% monoliths will be studied under Task 3 in kinetic studies at high temperatures (573 to 623 K).

2. Hydrogen Chemisorption Measurements

Hydrogen chemisorptive uptakes were measured on a few catalyst samples. These data are listed in Table 2. The hydrogen chemisorption data on Inco nickel powder confirmed earlier work on the stoichiometry of hydrogen adsorption on nickel. Using 0.068 nm^2 per nickel surface atom and 0.49 m^2/g BET surface area for the Inco powder the ratio of H/Ni_s is 0.9. While slightly lower than the previously reported value of 1.1, this is very close to the expected stoichiometric value of one hydrogen atom per surface nickel atom.

3. Sulfur Analysis

Our laboratory has developed a new method for quantitative measurement of sulfur on poisoned catalysts. In the past we used the method of Zutshi and Mahadevan (6) which incorporated a reducing acid solution and recovery of the sulfur in a cadmium acetate solution followed by reaction to form methylene blue. There were some modifications of this method by Fowler (7), who showed sulfur recovery of 90% of predicted levels.

Our new method consists of placing the poisoned catalyst in a strong reducing acid to reduce the sulfur to H_2S. Hydrogen is bubbled through the solution to purge the H_2S. The purge gas is analyzed at one minute intervals by gas chromatography using a flame photometric detector. Graphing H_2S concentration versus time and knowing the purge gas flow rate, the area under the curve yields the total weight of sulfur. For a totally sulfided catalyst sample this new method indicated 95% recovery of predicted sulfur.

This new method appears to produce accurate results. More studies are being performed to document its accuracy. Although this method takes more time, it is believed that more accurate results are thereby obtained.

4. Carbon Monoxide Chemisorption Measurements

During the past quarter, investigation of the formation of nickel carbonyl during CO chemisorption continued with testing of presulfided catalysts. The experimental method has been previously

Table 2

H_2 Chemisorption Uptake Data

Catalyst	Nominal Composition (wt.% nickel)	H_2 Uptake (moles/gram)
Pellets		
Ni-A-117	15	151
Powders		
Inco Ni #287	100	5.1
Monoliths		
Ni-M-188	0.5	7.5
Ni-M-195	0.1	2.2

reported (5). Data from these tests are listed in Table 3.

Runs performed on Sample I of 3% Ni/Al_2O_3 (runs 34I-41I) constitute a full set of the data points on a single catalyst sample. Run 34I gives an initial uptake of 30.6 μmoles/g. 35I and 36I give characteristic CO uptakes for this catalyst at the respective temperatures involved. Run 37I was a 2 hour sulfiding treatment involving sufficient H_2S in H_2 to poison approximately 50% of the metal surface area. As can be seen, the uptake did not decrease by 50%. Perhaps the previous measurements and pretreatments had the effect of further reducing the catalyst or changing its dispersion.

Run 39I shows a marked increase in the CO uptake which can be attributed to the presence of sulfur on the catalyst. Sulfur apparently catalyzes the formation of $Ni(CO)_4$. After this run, the catalyst as seen in the reactor, appeared much whiter than before indicating loss of Ni.

Run 40I shows a large CO uptake, but not as large as in Run 39I. This decrease is undoubtedly due to the removal of Ni from the catalyst in the process of $Ni(CO)_4$ formation. A final H_2 uptake shows only 8 μmoles/g of surface area level. The catalyst at this point was a light grey color as a result of removal of Ni from the surface.

In the next quarter we will analyze the catalyst and product effluent samples for amounts sulfur and nickel.

4. Electron Microscopy

A number of different catalysts were examined with the electron microscope during this quarter. Samples of Ni-S-101 (13.5% Ni) were sintered at 923 K and 1023 K for 51 hours and crystallite size distributions calculated from the resulting micrographs (Table 4). Bar graphs were prepared in order to visualize the effect of the temperature variation in sintering (Figure 2). A bar graph of Ni-S-101 sintered at 973 K and one of fresh Ni-S-101, both reported during the last quarter, were added for comparison.

The narrow distribution of the fresh sample began to broaden upon sintering. Two main peaks were evident when sintering occurred at 973 K with a more dominant peak forming when sintered at 1023 K. Tailing towards the higher diameter range was obvious when the distributions were compared together. The average particle sizes determined for all three temperatures sintered samples agreed very closely to those determined by H_2 chemisorption (Table 5).

Two models have been proposed for the sintering of a catalyst: (i) the migration of entire crystallites over the support surface resulting in collisions and ultimate coalescence of crystallites (crystallite migration); and (ii) the migration of detached atoms from one crystallite to another (atomic migration). Richardson and Crump (8) describe the two theories and their article contains excellent references for an in depth comparison of the theories.

Table 3

Carbon Monoxide Chemisorption Measurements at 273 and 298 K Before and After Sulfur Poisoning (3% Ni/Al_2O_3)

Run #	Temp K	Absorbate Gas	Uptake	CO/H	Sulfur poisoned[a]	Ni Detected
34I[b]	298	H_2	30.6			
35I	273	CO	121	2.0		No
36I[c]	298	CO	109	1.8		Yes
37I[b]						
38I[c]	298	H_2	23.2		Yes	
39I	273	CO	950	20.4	Yes	Yes
40I[d]	298	CO	314	6.8	Yes	Yes
41I[d]	297	H_2	8.0			

a Sample poisoned in a fluidized bed at around 725 ± 5 K in 10 ppm H_2S in H_2 until approximately 1/2 of the sites were covered. The flow rate of the 10 ppm H_2S mix was 280-300 cm^3/min. The amount of sample was 1.0 g.

b Additional 2 h reduction before chemisorption.

c Additional 3 h reduction before chemisorption.

d Additional 1 h reduction before chemisorption.

Table 4

Transmission Electron Microscopy Particle Size Distributions
Percent Particles in each Size Range

SAMPLE	Size Range nm <1	1.1-2.0	2.1-3.0	3.1-4.0	4.1-5.0	5.1-6.0	6.1-7.0	7.1-8.0	8.1-9.0	9.1-10.0	10.1-11.0	>11.1
Ni-S-101 fresh	0	8	80	10	1	1	1	0	0	0	0	0
Ni-S-101 923 K	0	5	48	23	10	12	1	0.5	0.5	0	0	0
Ni-S-101 973 K	0	0.3	25.2	16	9	27	8	5	6	1.8	1.4	0.3
Ni-S-101 1023 K	0	0.8	15	11	10	30	11	8	11	1.5	1.5	0.2
Ni-S-103 D = 14%	0	0	5	2	4	12	8	9.5	17	6	18	18.5
Ni-S-103 D ≈ 14%	0	0	1	5	5	11	7	8	18	6	18	21
Ni-S-103 D = 35%	0	16	73	9	1	1	0	0	0	0	0	0
Ni-S-104 D = 5%	0	22	58	4	2	3	0.4	1	1	0.2	1.4	7
Ni-S-104 D = 17%	0	23	46	4	3	6	2	2.5	5	1	3.5	4
Ni-S-104 D = 20%	0	12	46	10.3	8.3	11	2.3	3.4	3.4	0.7	1.4	1.2

Table 5

Comparison of Electron Microscopy and Chemisorption Particle Size

Catalyst	wt% Nickel	Pretreatment Duration	H_2 Adsorption[a]	% Dispersion[b]	H_2 Chemisorption[c]	T.E.M.[d]
Ni-S-101	13.5					
fresh			442	38	2.8	2.9
923 K		51 hrs	252	22		
973 K		51 hrs	178	15	4.4	4.1
1023 K		51 hrs	177	15	6.3	6.3
Ni-S-103	2.76					
calcined		573 K/1 hr	37	16	6.1	11.3
calcined		573 K/3 hrs	35	15	6.5	11.1
uncalcined			85	36	2.7	2.9
Ni-S-104	15					
calcined		773 K/22 hrs	61	4.8	20.2	19.4
uncalcined			217	17	5.7	9.7
uncalcined			258	20.2	4.8	6.9

[a]Based on total H_2 uptake at 298 K (in μmoles H_2/g catalyst).

[b]Calculated from H_2 uptake assuming 100% reduction.

[c]Particle sizes given in nm.

[d]Surface area averaged value from Transmission Electron Microscopy (in nm).

Figure 2. Crystallite Distribution

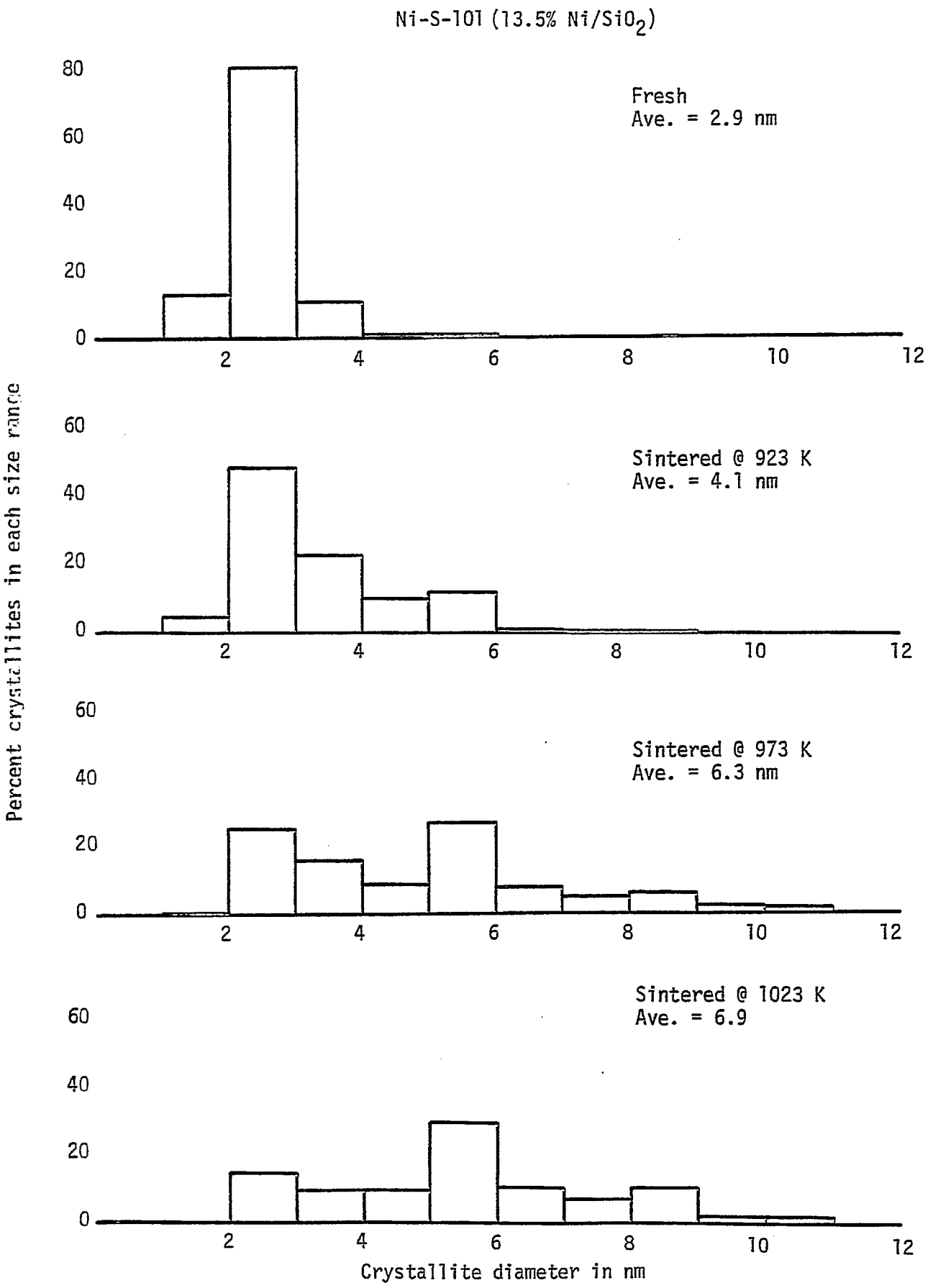

The tailing of the crystallite size distribution toward the higher diameter crystallites apparent after sintering at 923 K and still noticeable with the 973 K sintered sample is characteristic of crystallite migration whereas atomic migration generally predicts a "tail" in the small diameter range. However, it is important to note that a characteristic broadening of the distribution occurs in all three of the sintered samples. This is particularly noticeable in the 973 K sample and in the 1023 K sample with a stable crystallite size forming between 5 and 6 nm. The broadening in the distribution is representative of atomic migration and was expected in the samples sintered at higher temperatures. If crystallite migration was predominat at the higher temperatures larger crystallites would be forced to migrate. This would tend to quickly eliminate the smaller diameter particles and the more rapid formation of a higher diameter distribution. This is not evident in the distribution observed at 1023 K.

The sample sintered at 923 K tends to support both theories. Tailing is quite evident (crystallite migration), however, definite broadening of the distribution is observed.

This would suggest that both crystallite migration and atomic migration occur at the lower sintering temperature (923 K) or at least are indistinguishable. At 973 K tailing is still quite noticeable along with definite broadening of the distribution. Again both theories would seem to be playing a role in the changing distribution of the sample. At 1023 K it would appear that atomic migration is now predominant.

Ni-S-104 (15% Ni/SiO_2) and Ni-S-103 (3% Ni/SiO_2) samples were subjected to a variety of pretreatments, i.e. calcination at various temperatures in order to prepare samples with varying nickel dispersions. Dispersions ranging from D = 5% to D = 35% were obtained. Particle size distributions (Table 4) were calculated for these samples and average particle sizes varied from 2.7 nm for D =35% to as high as 19.4 nm for D = 5%. H_2 chemisorption averages were somewhat smaller than those obtained from E.M. and may be the result of some nickel particles not adsorbing H_2 but remaining visible, thus being detected by the electron microscope.

Samples of nickel on titania were photographed. Preliminary results show somewhat transparent crystallites with a 3% nickel sample suggesting tightly bound crystallites having a 2-dimensional raft-like structure (9). Figure 3 is a micrograph showing a side view of a nickel raft. A 15% nickel sample also exhibited thin, translucent crystallites, however, high contrast, high density crystallites were also observed.

Task 2: Activity Testing

No specific progress was made under this task during the past quarter. However, plans have been made to finish activity tests of monolithic nickel catalysts of different geometries during the next 2 quarters.

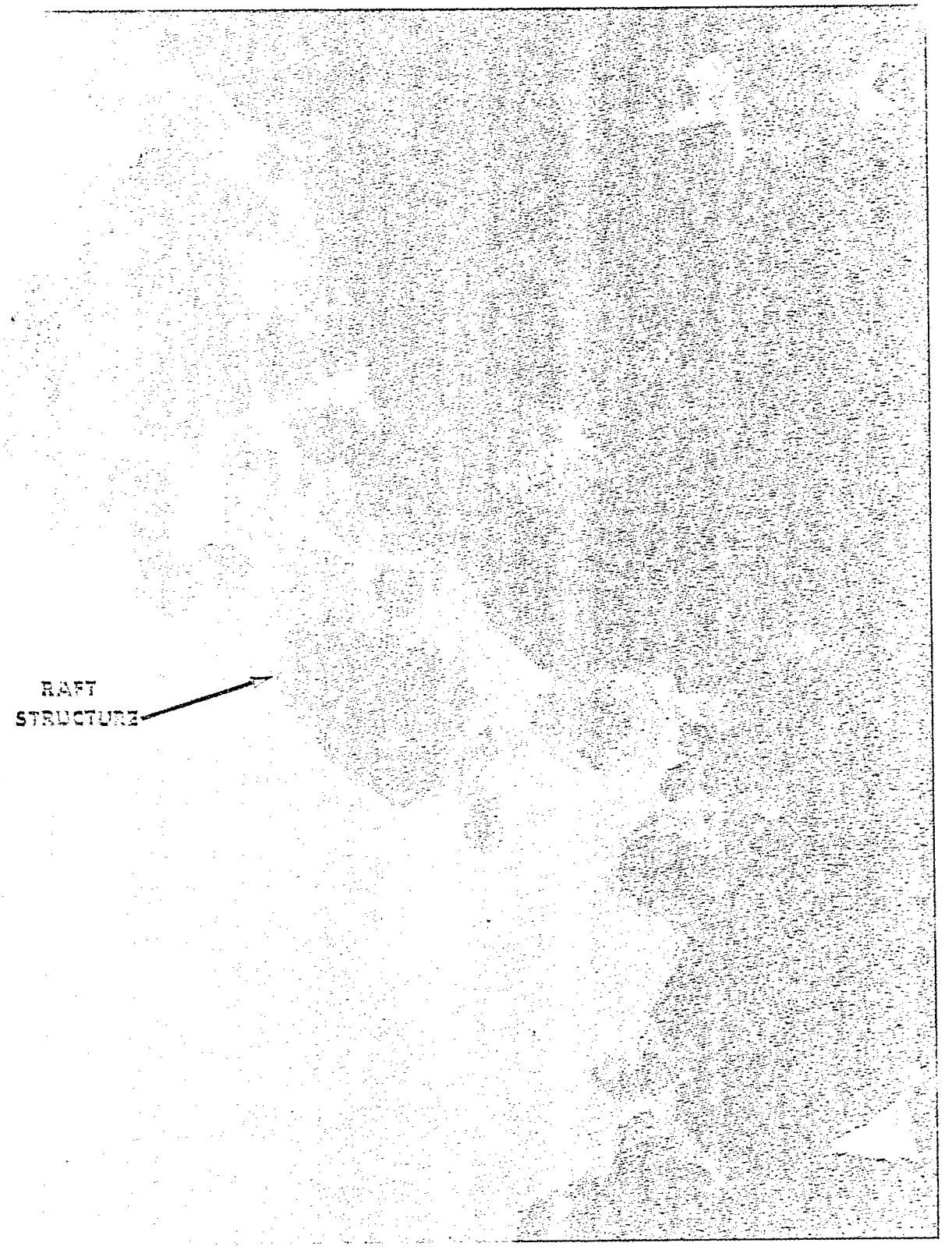

Figure 3. Electron Micrograph of 3% Ni on Titania.

Task 3: Kinetic Studies

a. Experimental Studies. Several catalysts were tested in the high pressure stirred tank (Berty) reactor. The first test was on Ni-A-177 and 15% nickel on alumina pellets. This test examined the decrease in catalyst activity at low temperature, 473 K and high pressure, 6900 kPa. The H_2/CO ratio was 3/1 and conversion was kept below 10%. After six hours, carbon monoxide conversion dropped 40% while methane production decreased only about 20%. The decrease in activity is apparently due to formation of C_{2+} hydrocarbons which remain on the catalyst. FID detection showed the presence of C_1, C_2, C_3 and perhaps C_4. The catalyst on examination after the test had the aroma of high molecular weight hydrocarbons.

The second test was made with 4.3% nickel on alumina pellets, Ni-A-123 at 523 and 623 K and 690 kPa. The purpose of this test was to provide data for comparison between pellet and monolith supports at high and low conversion. Data from a monolith catalyst with a comparable nickel loading will be tested under the same conditions next quarter.

Two monolith catalysts of low nickel loading were tested at higher temperatures. Ni-M-188, a 0.5% nickel on 10% alumina cordierite monolith catalyst was tested at 548 K and 6900 kPa. Despite a H_2/CO ratio of 3 the catalyst deactivated rapidly. At first it was thought that some oxygen must have entered the reactor system. However, the next test on Ni-M-195, 0.1% nickel on 2% alumina, in spite of extreme precautions taken to remove any oxygen from the reactor lines before test, rapid deactivation was again seen. Figure 4 compares the loss in activity for these two catalysts. The high partial pressure of carbon monoxide and the high temperature lead to rapid carbon deposition. The low loading catalysts also seem to be more susceptible to this deactivation. At the higher temperature more rapid and more extensive losses in activity occur.

An activation energy for the temperature range 573 to 623 K was determined on the Ni-M-195 catalyst before the pressure was raised to 6900 kPa and deactivation occurred. Figure 5 shows the data in the form of an Arrhenius plot. The activation energy is approximately 82 kJ/mole for $T < 608$ K. Above 608 K there is a shift in activation energy to 58 kJ/mole. This is in good agreement with the work by Polizzotti et al. (10) on nickel foils and powders. The very thin alumina coating and low loading on these monolith catalysts combined with the mixed flow reactor eliminate the possibility that mass transfer or intra-particle diffusional effects could be responsible for this lower activation energy.

In the next quarter monoliths of low metal loadings will be tested to determine the activation energy from 523 to 573 K with $H_2/CO = 3.0$ and from 523 to 623 K with $H_2/CO = 20$ at pressures of 690, 3500 kPa.

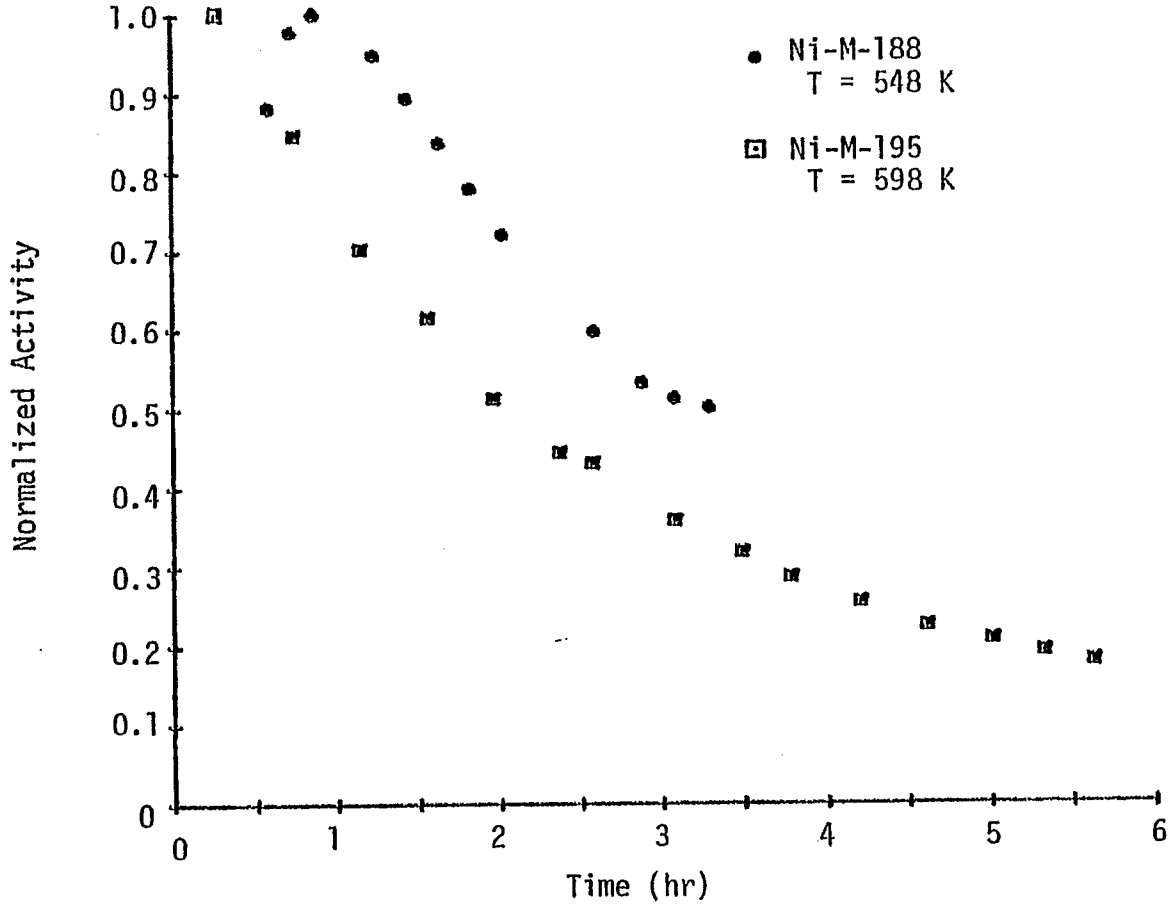

Figure 4. Loss of Activity at 6900 kPa

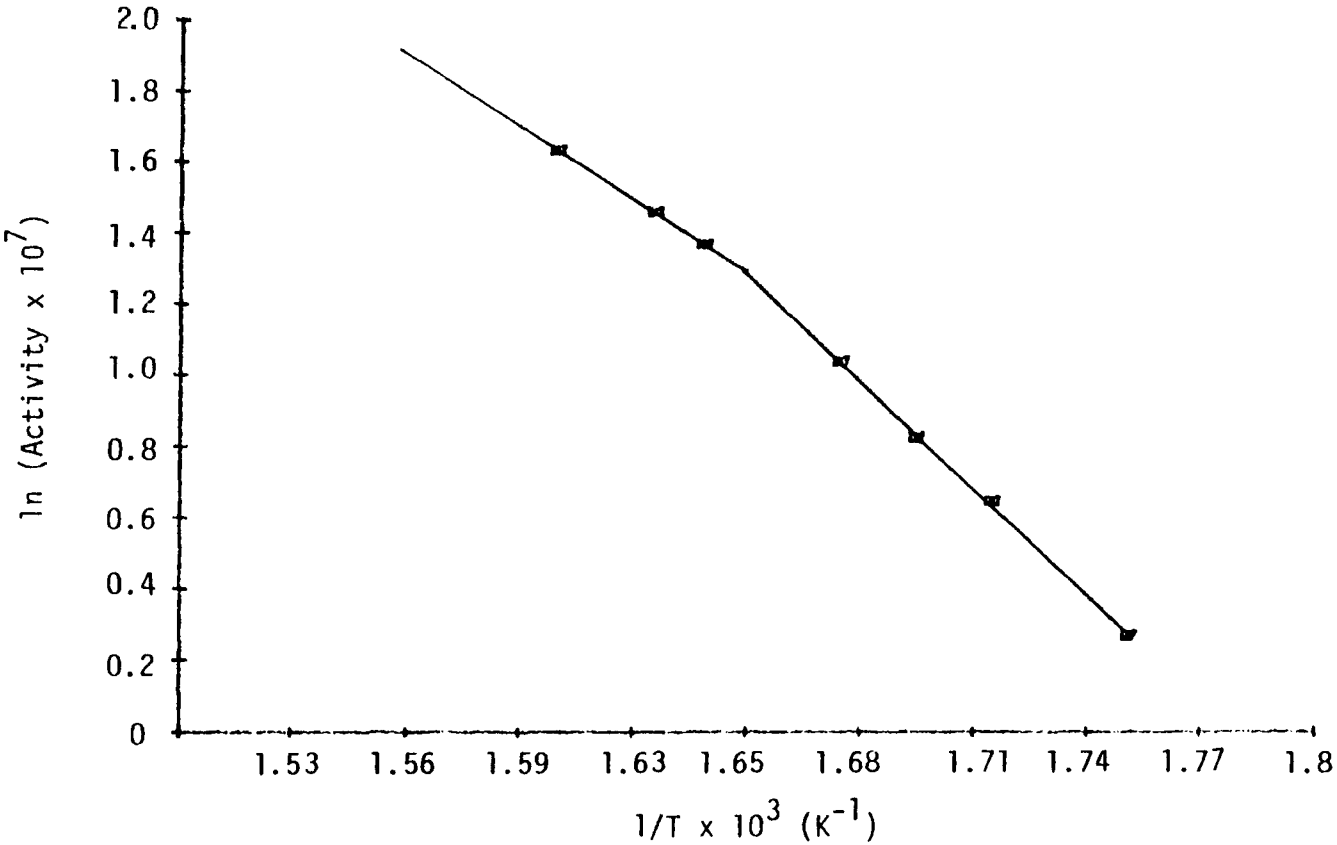

Figure 5. Activation Energy Ni-M-195.

Effects of total pressure and partial pressure will also be determined at 548 and 598 K and 690 to 3500 kPa. H_2O and CH_4 will be added to reactants in separate tests to determine product inhibition effects.

b. Computer Model. A one-dimensional computer model has been developed for methanation in nickel monolith catalysts. The assumptions leading to the development of the differential equations are given in Table 6, while the equations are listed in Table 7. The auxiliary equations for calculation of physical properties are presented in Table 8. Nomenclature is given in Table 9. The differential equations have been solved using Adams predictor-corrector numerical methods on a DEC-10 computer. The computer costs for this study were paid by a small grant from the BYU student research fund.

After initial program debugging and testing, the computer model was used to compare the solutions for several kinetic expressions to actual experimental data. Figure 6 shows the model's predictions using the empirical kinetic expressions for methane production given by Vannice (11). The correlation between the model and experimental values is very good for low conversions. At higher conversion, transport effects and these empirical methanation kinetics alone will not explain the reaction behavior. Product inhibition was next introduced into the kinetic expression. This produced much better correlation between the model and experimental data for conversion of CO up to 70%; at higher conversion discrepancies still remained.

The effects of introducing a competing reaction into the kinetic expression are shown in Figure 7. The kinetic expression for this competing reaction is an estimate of the water-gas shift reaction kinetics. The correlation between experimental and predicted values show that a competing water gas shift reaction could explain the reaction behavior throughout the conversion range.

The effect of changes on the various physical parameters of the catalyst and reactor were also studied. Figure 8 is an example where the results of changing H_2 uptake, nickel loading or catalyst activity are shown. It is interesting that the catalyst with lower activity not only reaches a lower maximum conversion but also requires a higher temperature to reach a maximum conversion. The competing reaction becomes more important with temperature. Thus optimization of methane production is not only a function of temperature but of catalyst activity and other reactor variables.

During the next quarter we plan to refine the computer model by including experimental water-gas shift kinetics, expanding chemical species equations to include CH_4, and CO_2, and H_2O and comparing the effects of channel size on reaction behavior.

Table 6
Model Assumptions

1. One channel in the monolith may be chosen as representative of the entire catalyst.

2. The monolith's channels are cylindrical and a cylindrical coordinate system may be used. This is partially true since the corners of the rectangular channels tend to be rounded by the alumina washcoat.

3. The density, thermal conductivity and diffusivity are constant for purposes of deriving the differential equations. However, these are later allowed to vary as function of temperature and composition.

4. The reactor and the catalyst are at steady state.

5. The channel is axially symmetric.

6. The effects of gravity are neglible.

7. All reactions in the reactor take place on the wall of the channel.

8. Axial diffusion and heat conduction are negligible relative to convective transport.

9. Radial velocity is small. No axial heat conduction in the solid.

10. The system can be described in terms of hydrogen and carbon monoxide. Other components may be neglected.

11. The gas phase is in laminar flow and free of developing flow effects.

12. Fourier's and Fick's law can be applied to radial diffusion and heat conduction. This can be later corrected for fluxes and high mass transfer rates.

Table 7

Computer Model - Basic Equations[a]

Equation of Continuity Chemical Species

$$\frac{\partial Y_{H_2}}{\partial Z} = \frac{2\,L\,K_{H_2}}{R\,\langle v\rangle}\left[Y_{H_2} - Y^{s}_{H_2}\right]$$

$$\frac{\partial Y_{CO}}{\partial Z} = \frac{2\,L\,K_{CO}}{R\,\langle v\rangle}\left[Y_{CO} - Y^{s}_{CO}\right]$$

Equation of Energy

$$\frac{\partial T}{\partial Z} = \frac{2\,L\,H}{C_p\,R\,\langle v\rangle}\left[T - T^{s}\right]$$

Boundary Conditions

At $r = R$

$$Y^{s}_{H_2} = Y_{H_2} - \frac{3\,RR}{K_{H_2}\,C^{i}_{H_2}}$$

$$Y^{s}_{CO} = Y_{CO} - \frac{RR}{K_{CO}\,C^{i}_{H_2}}$$

$$T^{s} = T - \frac{HR\,RR}{T^{i}}$$

At $z = 0$

$$Y_{H_2} = Y_{CO} = T = 1$$

---

[a]Nomenclature listed in Table 9.

Table 8

Auxiliary Equations[a]

Velocity

$$\langle v \rangle = \frac{SV}{3600} \times \frac{CV}{POR} \times \frac{P}{R_G} \times \frac{273}{T}$$

Density

$$\rho = \frac{AMW \times P}{R_G \times T}$$

Heat Capacity

$$C_p = \sum_i \frac{z_i}{x_i} C_{pi} \qquad i = H_2, CO, H_2O, CH_4$$

$$C_p = 6.947 - 2.0 \times 10^{-4} T + 4.81 \times 10^{-7} T^2$$

Diffusion Coefficient

$$D_{CO\text{-}N_2} = \frac{3.7585 \times 10^{-5} \, T^{1.5}}{P \times \Omega}$$

Mass Transfer Coefficient

$$K_{CO} = D_{CO\text{-}N_2} (1.48) \, R \left(1 + \frac{.095 \times 4R^2 \times \langle v \rangle}{D_{CO}}\right)^{.45}$$

K_H, D_H = similar to K_{CO} D_{CO}

Knudsen Diffusion

$$DK_{CO} = 1.010 \times 10^{-3} \, T^{.5}$$

Viscosity

$$U = \frac{1.024 \times 10^{-5} \, T^{.5}}{\Omega}$$

Thermal Conductivity

$$KT = U \times [C_p + 2.484]/28$$

Heat Transfer Coefficient

$$H = \frac{1.48 \, KT}{R}$$

$$HR = 45{,}122.8 + 16.624T - 3.14 \times 10^{-3} T^2 + 1.755 \times 10^{-6} T^3$$

$$RR = A e^{-\frac{E}{RT}} C_{H_2}^{\,a} \, C_{CO}^{\,b}$$

[a]Nomenclature listed in Table 9.

Table 9

NOMENCLATURE

AMW	Gas average molecular weight
Cp	Heat capacity
C	Concentration
CV	Catalyst Volume
H	Heat transfer coefficient
HR	Heat of reaction
K	Mass transfer coefficient
KT	Thermal conductivity
L	Channel Length
P	Pressure
POR	Catalyst porosity - % Cross sectional area open to flow
r	Radial direction
R	Channel radius
RR	Kinetic rate expression
T	Dimensionless temperature
V	Viscosity
Y	Dimensionless concentration
x	Mole Fraction
Z	Dimensionless length

SUPERSCRIPT

a,b	reaction orders
i	initial values
s	surface values

Table 9 (cont).

SUBSCRIPT	
H	Hydrogen
CO	Carbon monoxide

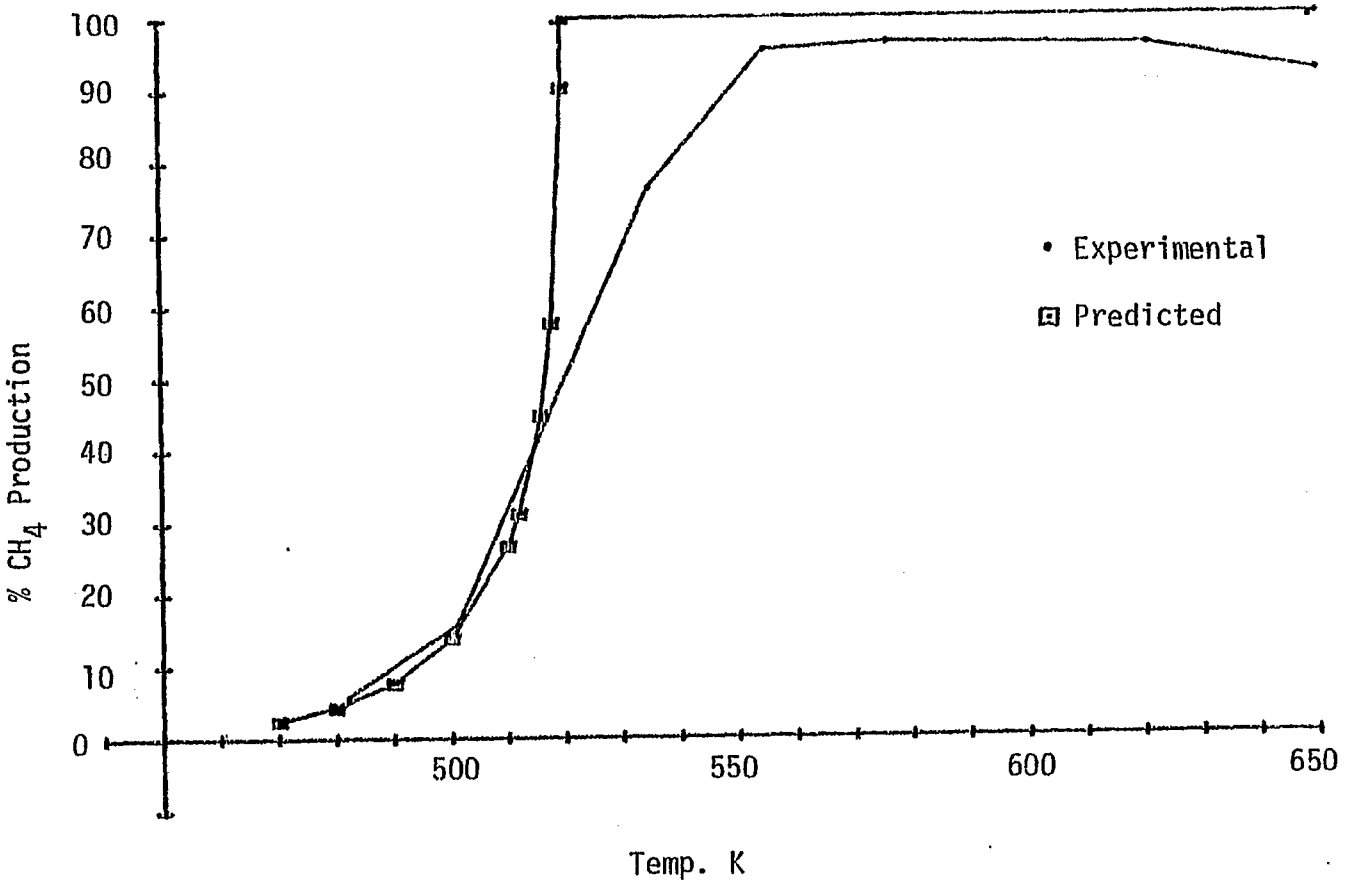

Figure 6. Comparison of Experimental Results with Calculations from a Power Rate Law Model. Space Velocity = 43,000, P = 1300 kPa, H_2/CO = 4.4/1.

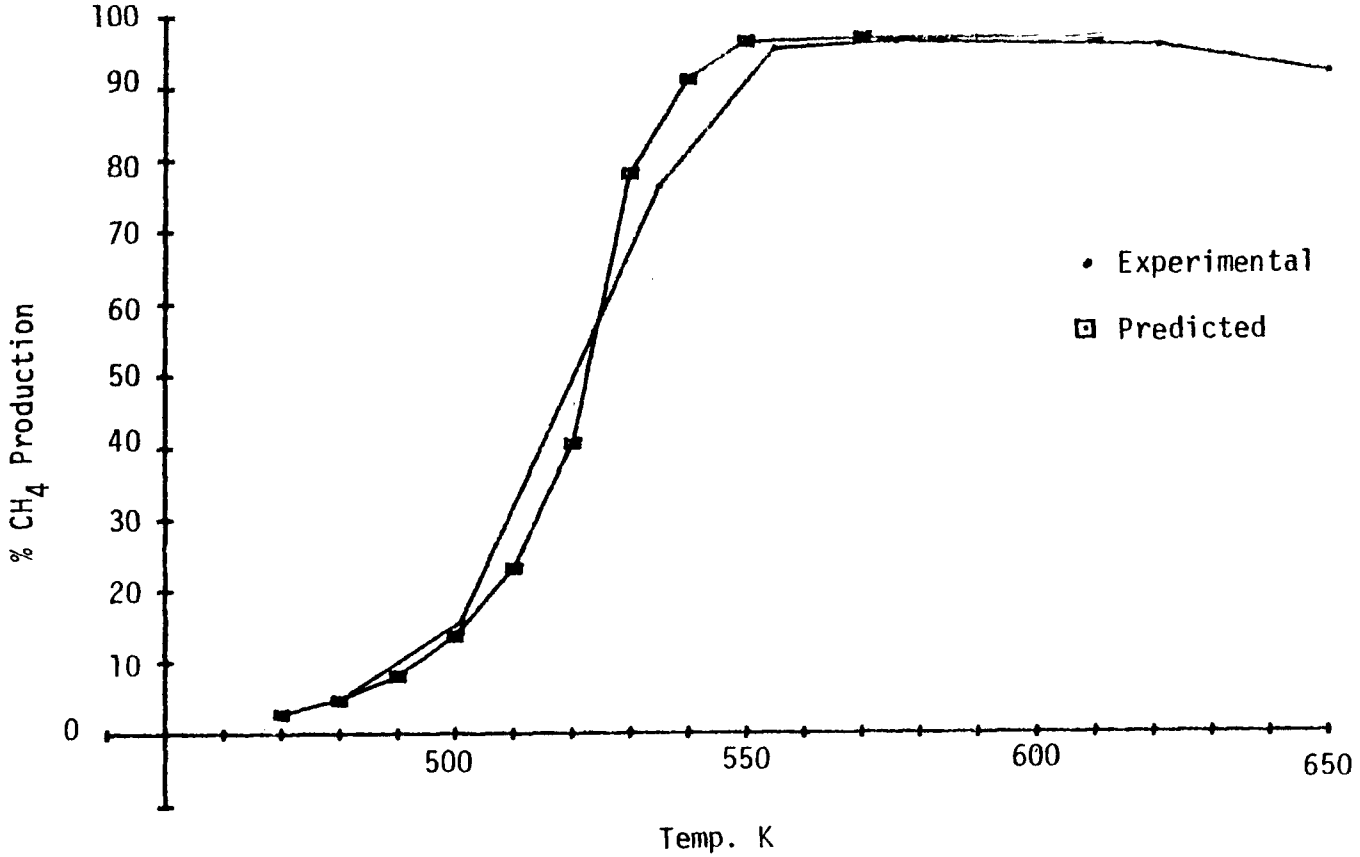

Figure 7. Comparison of Experiment and Calculation Results Based on a Langmuir Hinshelwood Competing Reaction Model.

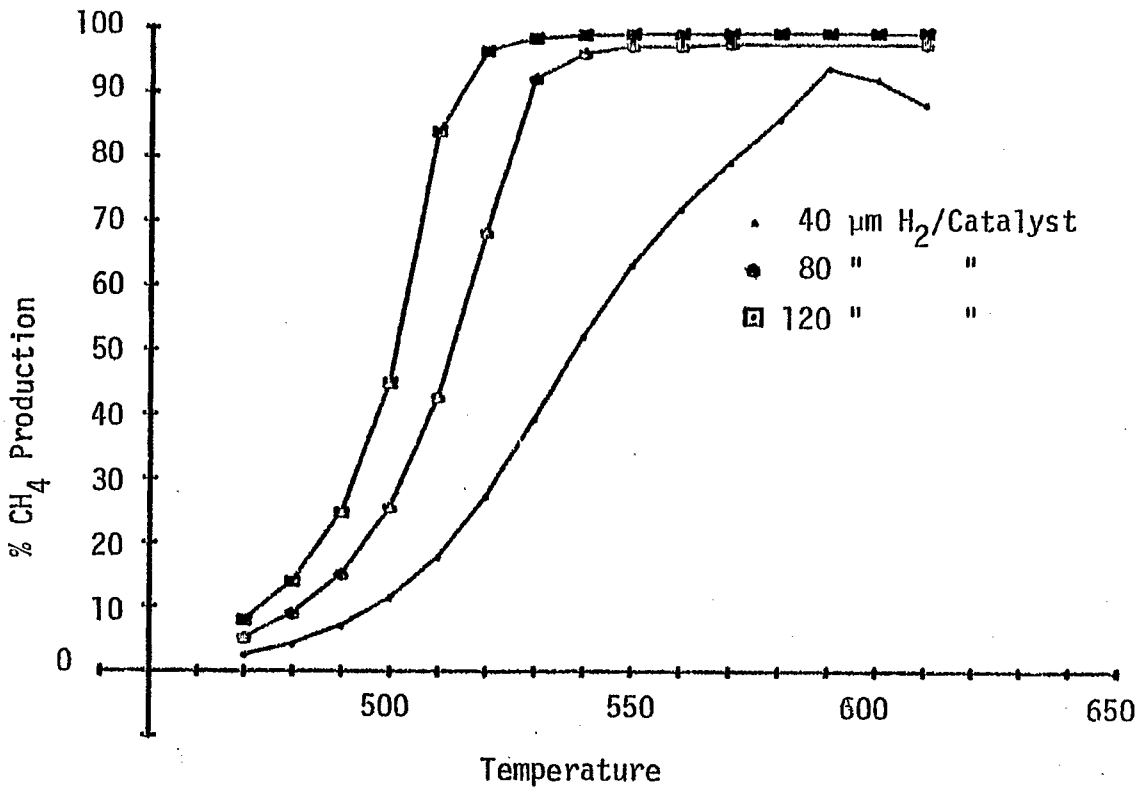

Figure 8. Comparison of Increased Ni Surface Area on Catalyst Performance. Space Velocity = 30,000 h^{-1}, H_2/CO = 3/1, P = 1030 kPa.

Task 4: Degradation Studies

During the past quarter we discovered some very important limitations to the quartz internal recycle reactor. We wrote a short letter to Industrial and Engineering Chemistry: Fundamentals, the major points of which are summarized below.

We would like to clarify several issues raised in the recent correspondence of Berty (12) and the article by Fitzharris and Katzer (4). We find that an all-glass internal recycle reactor has limited but very useful application in kinetic and poisoning studies of real catalysts -- particularly monolithic catalysts.

Our quartz internal recycle reactor is of the same design as that described by Fitzharris and Katzer (4). We confirmed ideal-mixing behavior of the reactor by transient response tests. We were also able to reproduce methanation turnover numbers and activation energies on supported nickel in pellet, powder and monolithic form with 20-25% of those obtained in tubular reactors and within a factor of 2 compared to data from the literature (see Table 10).

Berty criticized the all-glass reactor commenting that at low pressure the glass impeller may not develop sufficient pressure head to cause significant flow through a bed of catalyst particles. Based on pressure drop calculation, he predicted a flow through a single particle diameter deep bed in the glass reactor of about 0.2 m s^{-1} (at 103 kPa and 1000 RPM) approximately 1/6th the flow needed to produce incipient turbulence. We checked this experimentally by means of a hot-wire anemometer for flow developed by the stirring unit at ambient pressure (86 kPa) through monolithic and particulate catalysts. We also calculated flows using Berty's equations for comparison with our experimental data measuring air flows. Table 11 shows the calculated and measured flows.

In the case of the particulate catalysts, the measured flows are a factor of 10 less than calculated values. We believe the lower than expected flow can be attributed to the thin layer of quartz wool used to support the particulate samples. Comparison of the measured flow with the outlet flow indicates a recirculation ratio of one for the particulates. However, for the monolithic catalyst the measured flow is only a factor of 3 lower than the calculated value; this is anticipated since the length of the bed exceeds the hole size by about a factor of 3. Moreover, the observed recirculation ratio is 15 for the monolith. Thus a reasonable flow with considerable recycle can be developed through the monolith but not through the particulate samples. In actual operation, higher flows and recirculation ratios would be possible since the reactor can be pressurized to obtain at least a factor of 2 increase in pressure with a proportional increase in pressure head. Moreover, the depth of the monolithic bed could be decreased by at least a factor of 2-3. In other words, it is possible to obtain flows of 0.5-0.6 m/s through a monolithic catalyst bed in the all-glass reactor.

Table 10

Comparison of Methanation Turnover Numbers at 500 K

Catalyst	Turnover Number x 10^3 molecules CH_4 produce/site sec
All-glass Internal recycle	
6% Ni on Al_2O_3 powder	3.2
6% Ni on Al_2O_3 pellets	3.1
3% Ni on Al_2O_3 monolith	2.2
Tubular Fixed-Bed Reactors	
6% Ni on Al_2O_3 spheres[a]	2.5
5% Ni on Al_2O_3 powder[b]	1.0

[a] Jarvi, G.A., Mayo, K.B. and Bartholomew, C.H., To be published in Chem. Eng. Commun., 1979.

[b] Vannice, M.A., J. Catal. 37 449 (1975). Calculated using his rate expression and activation energy.

Table 11

Flows in the Quartz Internal Recycle Reactor

Catalyst	Calculated Flow[a] of Air (in/sec)	Measured Flow or Air (m/sec)	Recirculation Ratio
40 mesh Al_2O_3[b]	0.20	0.02	1
0.32 cm diam. Al_2O_3 pellets	0.20	0.02	1
cordierite monolith 46.5 □/cm^2 (1 cm long x 2.5 cm diam)	0.33[c]	0.10	15

[a] Using the equation of Berty (1979) and 1000 rpm.

[b] Supported on a 1-2 mm layer of quartz wool.

[c] Using the pressure drop expressions of Hegedus, L.L. ACS Chicago meeting, p. 487, August, 1973.

Berty suggested that a velocity greater than 1.4 m s^{-1} is desirable to obtain turbulent flow in a catalyst bed. The implication is that turbulent flow is needed to avoid non-ideal flow patterns which adversely affect the measurement of reaction rates. However, our experimental results in Table 10 suggest that this is not a serious problem for our thin beds and particular reaction conditions. Presumably if laminar flow patterns were affecting the rate measurements, a change in flow direction through the reactor (particularly of the Fitzharris-Katzer deign) would reveal this; however, upon reversing the inlet and outlet streams, the rates and conversions were found to be the same (within $\pm$ 3-5%). Perhaps in thin catalyst beds, entrance effects and developing laminar flow serve to produce plug-flow-like patterns.

Thus our experience agrees with Berty's suggestion that the all-glass recycle reactor is limited primarily to the study of films and thin catalyst beds (particularly monolithic beds) at low pressure. Nevertheless, we think it has broader application than he implied. It is in our opinion a convenient, low cost tool for obtaining accurate kinetic and poisoning data of practical as well as theoretical value for almost any real catalyst, because in principle any solid catalyst can be prepared in monolithic form (13). In addition, the quartz reactor enables sulfur poisoning studies to be conducted at low, but industrially-relevant poison concentrations (e.g. 0.001 to 1 ppm H_2S) where essentially all practical metal systems and even Pyrex introduce serious adsorption and/or contamination problems (14,4). Moreover, the use of monolithic catalysts provides an additional important advantage over particulate forms in kinetic studies - namely significantly lower pore diffusional resistance enabling intrinsic rates to be measured over a wide range of temperature and pressures using either glass and metal tubular reactors (15) or glass and metal internal recycle reactors (5).

Because the quartz reactor produces a questionably low flow through powdered catalyst samples, data obtained during the eighth quarter on Inco nickel powder and powdered Ni-A-120 are not reported.

Task 5: Technical Interaction and Technology Transfer

The principal investigator, Dr. Bartholomew, attended the 3rd International Conference on the Chemistry and Uses of Molybdenum held August 19-23 at the University of Michigan in Ann Arbor, at which he presented a paper on "Molybdenum-Based Methanation Catalysts" based in part on work supported by this contract. There were quite a number of other papers dealing with catalysis, especially in the area of hydro-desulfurization.

He also attended the DOE sponsored Conference on University Coal Liquefaction Contract Research held in Pittsburgh, September 6-7. This meeting provided opportunities to hear of recent developments in direct and indirect liquefaction and to meet Mr. Henry Pennline, who will be Contract Officer on our new contract (effective 9/19/79) to study selectivity and sulfur poisoning in Fischer-Tropsch synthesis.

During the quarter, the above mentioned note to I & EC Fundamental was submitted and a publication on H_2 and CO adsorption was prepared. Several other publications relating to this contract are in preparation.

IV. CONCLUSIONS

1. The activation energy of methanation over nickel decreases above 573 K from 82 to 58 kJ/gmoles at 700 kPa and $H_2/CO = 3$. This data was determined in Berty reactor and a monolithic catalyst so that mass transfer and intraparticle diffusion effects do not account for this shift in activation energy.

2. A one-dimensional computer model of methanation over monolithic catalysts was developed. This model shows that competing reactions such as water-gas shift affect maximum conversion and help explain the decrease in methane production at higher temperatures.

3. The sintering of nickel catalysts appear to take place by both crystallite and atomic migration methods at lower temperatures. However, electron microscope data suggest that atomic migration predominates at 1073 K.

4. The quartz internal recycle reactor developed by Fitzharris and Katzer has excellent application for poisoning studies on monolithic catalysts. However, pellet and powdered catalysts beds are not suited for poisoning studies in this reactor.

5. A new method for sulfur determination of poisoned catalysts appears to be more accurate and possibly more convenient than wet chemical techniques.

V. REFERENCES

1. M. Greyson, "Methanation" in "Catalysts" Vol. IV., ed. P.H. Emmett, Rheinhold Pub. Corp., New York (1956).

2. G.A. Mills and F.W. Steffgen, "Catalytic Methanation," Catalysis Reviews 8, 159 (1973).

3. C.H. Bartholomew, "Alloy Catalysts with Monolith Supports for Methanation of Coal-Derived Gases," Final Technical Progress Report FE-1790-9 (DOE), (Sept. 6, 1977).

4. W.D. Fitzharris and J.R. Katzer, Inc. Eng. Chem. Fundam. 17, 130 (1978).

5. C.H. Bartholomew, "Alloy Catalysts with Monolith Supports for Methanation of Coal-Derived Gases," Quarterly Technical Progress Report FE-2729-7 (DOE), (July 5, 1979).

6. Zutshi, P.K. and Mahadevan, T.N., Talanta 17, 1014 (1970).

7. Fowler, R.W., Master's Thesis, Brigham Young University, 1978.

8. Richardson and Crump, J. Catal. 57, 417 (1979).

9. E.B. Prestridge, G.H. Via, and J.H. Sinfelt, J. Catal. 50, 115 (1970).

10. Polizzotti, R.S., Schwarz, J.A. and Kugler, E.L., Symposium on Advances Fischer-Tropsch Chemistry, ACS Division of Petroleum Chemistry, Anaheim Meeting, March, 1978.

11. M.A. Vannice, J. Catal. 37, 449 (1975).

12. J.M. Berty, Ind. Eng. Chem. Fund. 18, 193 (1979).

13. Deluca, J.P. and Campbell, L.E., "Monolithic Catalyst Supports," in Advanced Materials in Catalysis, Acad. Press, New York, 1977.

14. Fitzharris, W.D. and Katzer, J.R., Paper submitted to J. Catal., 1979.

15. Jarvi, G.A., Mayo, K.B. and Bartholomew, C.H., to be published in Chem. Engr. Commun., 1979.

☆U.S. GOVERNMENT PRINTING OFFICE 1980-640-258/2131

U.S. DEPARTMENT OF COMMERCE
Technology Administration
National Technical Information Service
Springfield, VA 22161 (703) 605-6000